J. Water Environ. Nanotechnol., 6(3): 232-240 Summer 2021

ORIGINAL RESEARCH PAPER

Carbon Nano Particles as better Adsorbent against Photocatalytic Degrader for the Rhodamine-B Dye

Vatchalan Latha [*] **, *Selvam Pandiselvam***

Department of Chemistry, Sri. S.Ramasamy Naidu Memorial College, Sattur, India

Received: 2021-04-29 Accepted: 2021-06-13 Published: 2021-07-01

ABSTRACT

Paper industries will be using different kinds of dyes for producing various kinds of paper. Rhodamine–B (Rh-B) dye is one of the major sources of color effluents from textile and paper dyeing industries, and they cause long-term effects on an aquatic environment. So this work mainly focused on the synthesis of carbon nanoparticles from neem leaves, characterization, and its adsorption and photocatalytic action against Rh-B dye. In this study, Carbon nanoparticles (NPs) from neem leaves were synthesized for adsorption and photocatalytic degradation of Rh-B dye used in paper industries. The synthesized carbon NPs were characterized by the powder X-Ray Diffraction and Scanning Electron Microscopy. The adsorption and photocatalytic properties of carbon NPs were examined for 1 hour by studying the degradation of the Rh-B dye at every 5 minutes time interval through a UV-Visible spectrophotometer. The results obtained show that carbon NPs acts as better adsorbents than photocatalysts.

Keywords: *Adsorption, Carbon Nanoparticles, Dye Degradation, Photocatalytic activity, XRD*

How to cite this article

Latha V., Pandiselvam S. Carbon Nano Particles as better Adsorbent against Photocatalytic Degrader for the Rhodamine - B Dye. J. Water Environ. Nanotechnol., 2021; 6(3): 232-240.

DOI: 10.22090/jwent.2021.03.004

INTRODUCTION

Water is one of the most important natural resources for the existence of life. In many countries, most water sources are untreated. The major causes are untreated sewage, industrial effluents, the dumping of garbage, open sewage drains, and a lack of sufficient sewage treatment plants. Usage of untreated water causes low to high severe effects to water sources, soil resources, and living beings. The major part of pollution is from industrial wastes due to the usage of organic and inorganic dyes [1]. The commonly employed dye substances in paper industries[2] are Acid orange, Brown dye, Red dye, Paper yellow, Methylene Blue, Victoria Pure Blue, Malachite Green Crystals, Methyl Violet, Rhodamine-B, Auramine O [3].

Out of these, Rhodamine-B ($C_{28}H_{31}ClN_2O_3$) (Fig.1) is a xanthene cationic dye, which functions as a water tracer fluorescent. It is used as a staining fluorescent dye[4]. It is severely harmful when swallowed, with acute oral toxicity, causes serious eye damage or irritation, hazardous to the aquatic environment with long-term side effects[5,6].

Rh-B is an organic chloride salt having N-[9-(2-carboxyphenyl)-6-(diethylamino)-3H-xanthen-3-ylidene]-N-ethyl ethanaminium as the counterion.

Even at low concentrations, these Rh-B dyes can be harmful and they cause long-term effects for an aquatic environment and also human health. Therefore high-priority environmental research attention has been evolved to develop an alternative solution removing these organic pollutants [7] from the aqueous solution[8-9]. The possible methods are precipitation, adsorption, photocatalytic degradation, ion exchange, reverse

* Corresponding Author Email: *latha@srnmcollege.ac.in*

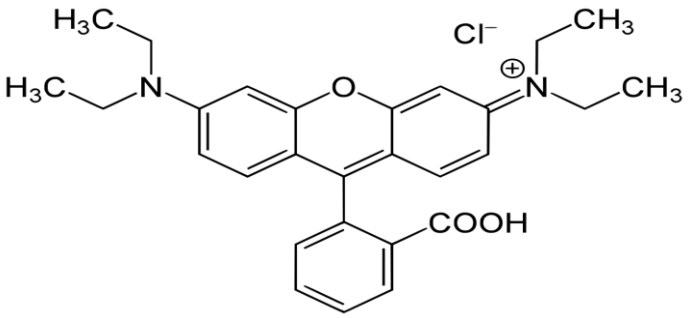

Fig. 1 Molecular Structure of Rhodamine – B Dye

osmosis, solvent extraction, and chlorination [10].

Among many of the dye effluent removal methods, adsorption is gaining more attention due to its low energy consumption, high selectivity at a molecular level, potential efficiency, and ability to separate various chemical compounds. Especially, adsorption of dyes [11] by activated carbon and its composites is one of the simplest and most economical ways of removing Rh-B dyes from wastewater.

Earlier studies [12-13] reported that photocatalytic activity has proven its performance in degrading the persistent organic dye pollutants with the help of light absorption in the water [14-15]. However, photocatalytic degradation performance depends on various factors such as composition and its microstructure, size, and surface morphology. In recent days, nanomaterials are used as a photocatalyst to degrade organic pollutants [16-17]. Even tiny nanoparticles are capable to form active sites of support materials through oxide-support interaction [18]. This would increase the overall surface area of the photocatalyst, and the support materials can act as a sink of electrons. Carbon-based nanoparticles are photocatalysts, but there is some limitation due to which they were not used commercially applications [19-21].

The Neem tree (Azadirachta indica A. Juss) is a tropical evergreen tree. For many decades, the neem tree is traditionally popular for its medicinal value. In Asia, beyond the wide usage at the Indian subcontinent, the neem tree products are efficiently used by various African countries as a remedial resource for therapeutics, preservatives, and insecticides. Also, neem leaves are the natural source of chemical compounds like flavonoids, polyphenols, isoprenoids, sulfur, and polysaccharides, which play an important role in scavenging the free radical. Neem leaf is the best source of medicinal treatments for eye disorders, bloody nose, intestinal worms, stomach upset, skin ulcers, fever, diabetes, gum disease, and liver-related issues.

It is mandatory to treat industrial effluents for a healthy future. Hence, in this work, a proposal for utilizing the carbon NPs synthesized from neem leaves to remove Rh-B dye is presented by adsorption and photodegradation methods.

MATERIALS AND METHODS

Synthesis of Carbon Nanoparticles

Carbon NPs are synthesized from Neem leaves as depicted in Fig 2. Initially, fresh neem leaves are collected; cleaned with distilled water and then these washed leaves were soaked in dilute hydrochloric acid (0.1N) for about 3-4 hours. After the soaking process, the color of the neem leaves was turned black. These black leaves are dried in a hot air oven at 120°C for 3-5 hours. The dried powder was collected and preserved for further analysis.

Adsorption study on Rh-B dye

In this work, the Rh-B dye is chosen for adsorption study [22-23] and its chemical structure is shown in Fig. 1. Using the decreased UV absorbency of the Rh-B solution, the adsorption performance of the carbon NP was estimated. The concentration of the Rh-B solution prepared for adsorption was maintained at 5 ppm. Then, 100 ml Rh-B solution is sonicated with 5mg of the synthesized carbon nanoparticle to gain better adsorption activity. Now, for 1 hour at a regular time interval (every 5 min), the absorbance of the Rh-B solution was measured by using a UV-Vis spectrophotometer.

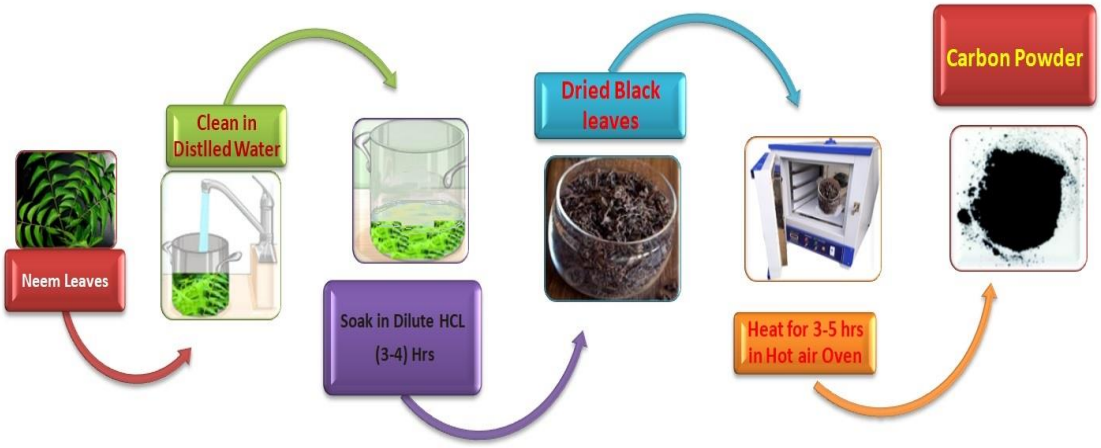

Fig.2 Process cycle of synthesis of Carbon Nanoparticle

Photocatalytic study on Rh-B dye

The photocatalytic activity of carbon NPs was conducted by the degradation of Rh-B dye as the model of pollutants under UV light irradiation [24-25]. The solution containing photocatalysts was exposed to UV irradiation during this activity by using four visible fluorescent lamps and four UV fluorescent lamps. Now, 75 mL of the Rh-B dye solution with 5 ppm concentration was sonicated continuously with 5mg of carbon nanoparticle in a 100 mL cylindrical Pyrex vessel reactor. This reaction was initiated by energizing the light source. During this process, for 1 hour at a regular time interval (every 5 min), a 5ml of dye solution resulted in 10 solution samples. To examine Rh-B's degradation, the UV-Vis spectra of the collected samples were recorded in the air atmosphere at room temperature by using a double beam UV-Vis spectrometer (Model UV-100 Super spec).

Characterization of synthesized carbon NPs

To characterize the surface morphology of the synthesized carbon NPs, the Scanning Electron Microscope (SEM)-EVO18 (CARL ZEISS) was used. SEM is a popular method for scanning the surface with a focused electron beam to create high-resolution imaging of the surfaces. This SEM can be employed to characterize the nano-scale materials too. The collected carbon NP samples were placed in an evacuated chamber and scanned in a controlled pattern by interacting with an electron beam. As a result of the interaction of this electron beam with the carbon NPs, it produces the SEM images of carbon NPs.

X-ray diffraction (XRD) is one of the most extensively used techniques for the characterization of NPs. Most commonly, X-ray diffractometer D8 Advance ECO (Bruker) is used to study the grain size of carbon NPs. This XRD can distinguish the crystalline structure based on the nature of the phase, lattice parameters, and crystalline grain size. The nanocrystalline size of the grain is evaluated by using the Scherrer equation [26-29] by broadening the most intense peak of an XRD measurement for a specific sample. The crystallite size here corresponds to the size of the grains of carbon NPs for the respective diffraction peak.

RESULTS AND DISCUSSION

SEM Analysis of carbon NPs

Based on the morphological studies of the synthesized carbon NPs with SEM analysis, the resultant SEM image was obtained through the interaction of electron beam with carbon NPs as depicted in Fig.3. It is observed that the synthesized carbon NPs formed a well dispersed and evenly distributed surface morphology structure in all directions. From this observed result, it can be shown that the synthesized carbon NPs have a smooth and uniform surface. This study further examined that, there is no contamination present with the carbon NPs.

XRD Analysis of carbon NPs

The crystalline structure of the synthesized carbon NPs in terms of XRD pattern analysis was

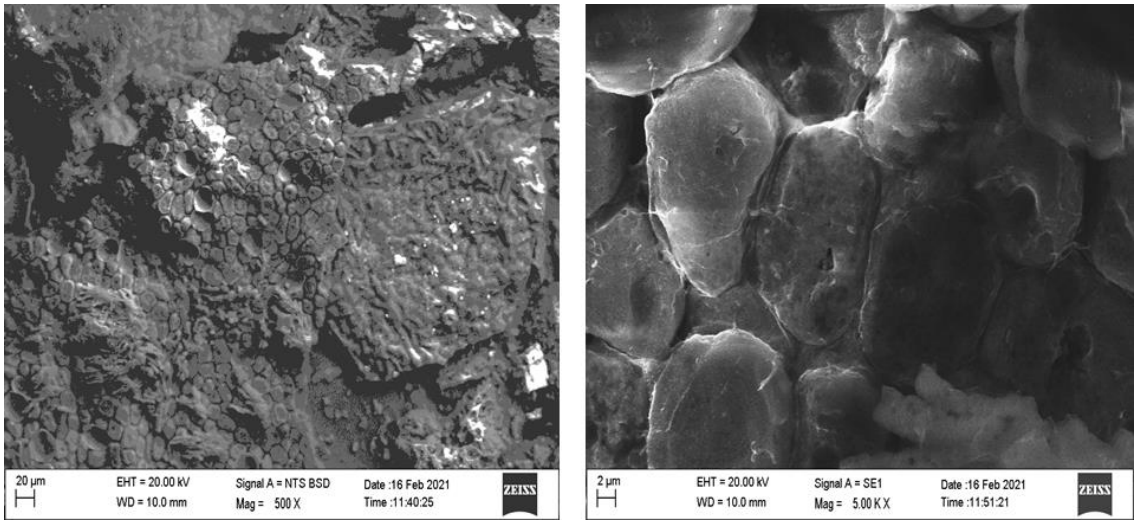

Fig. 3 SEM images of Carbon NPs

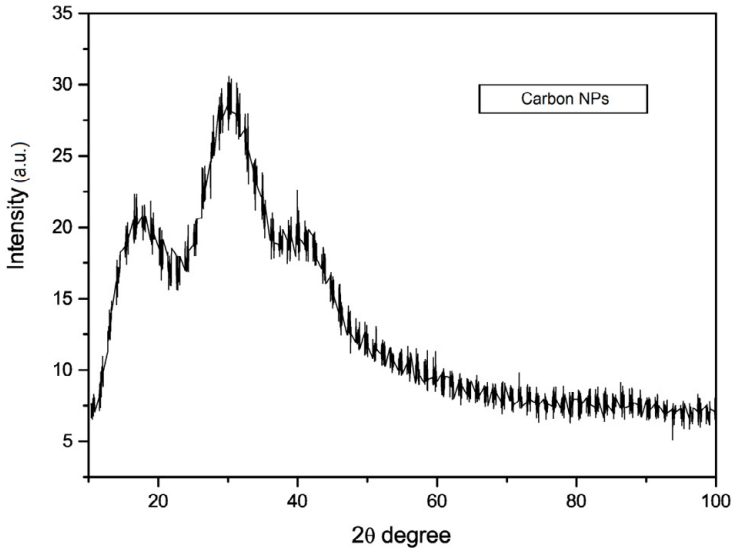

Fig. 4. XRD Pattern of Carbon NPs

portrayed in Fig.4.

As depicted in Fig. 4 for the synthesized carbon NPs the XRD pattern was observed with 2θ values. The diffraction angles such as 16°58`, 18°93`, 30°15`, 39°96`, are indexed to the 221, 100, 111, 220 crystal planes. The average size of the synthesized carbon NPs was calculated using the following Scherrer's equation [26-29].

$$D = \frac{k\lambda}{\beta\cos\theta} \quad (1)$$

where, D – Particle in size,

k – Scherrer's coefficient,

λ – Wavelength of the X-ray source (1.5406nm),

β – Full-Width Half Maximum (FWHM) and

θ – diffraction angle

Based on Scherrer's equation, the average size of carbon NPs is estimated as 6.78nm. This XRD analysis further helped to prove that synthesized carbon NPs are spherical by utilizing the indexed crystal planes.

Adsorption of dye pollutant by carbon NPs

For adsorption activity, the adsorption of Rh-B dye pollutant by the synthesized carbon

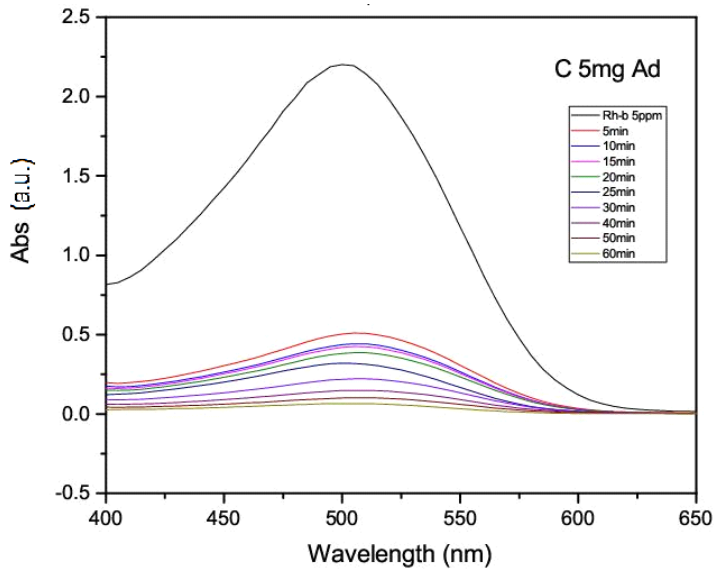

Fig. 5 UV – Visible spectra of Rh-B with C NPs at a time interval of 5 minutes from 0 to 60 minutes by adsorption studies

Table 1.The absorbance value with the concentration of the solution for adsorption and photocatalytic processes

S.No	Time (min)	Adsorption		Photocatalytic Activity	
		Abs (a.u.)	Conc (%)	Abs (a.u.)	Conc (%)
1	0	0	100	0	100
2	5	0.510	23.17	0.592	26.9
3	10	0.443	20.13	0.542	24.63
4	15	0.425	19.31	0.480	21.81
5	20	0.387	17.58	0.436	19.81
6	25	0.319	14.49	0.384	17.45
7	30	0.222	10.09	0.326	14.81
8	40	0.149	6.77	0.272	12.36
9	50	0.102	4.63	0.229	10.40
10	60	0.066	3.00	0.130	5.91

NPs was examined using UV–Vis spectra. During this examination, the adsorption peaks of the synthesized carbon NPs on the collected Rh-B solution samples were illustrated in Fig.5. Up to 30 minutes, the activity was measured at 5 minutes time interval. Then the interval is increased to 10 minutes, till the end. After 5 minutes the concentration of the dye solution is 23.17% and the absorbance maximum is 0.510 (Table 1). But this value constantly decreases. After 60 minutes, the intensity of absorbance reaches 0.066, nearly 0 and the corresponding concentration is 3% only.

From the spectra, it is distinguishable that the intensity of the characteristic peak of Rh-B observed at 500nm decreases concerning the time after adsorption with the synthesized carbon NPs. The adsorption of the Rh-B by the carbon NP can be visualized manually through the color degradation by seeing Fig. 6. The Rh-B dye is degraded to 97% after 60 minutes. The degradation percentage of Rh-B dye has been calculated using equation (2) with Beer-Lambert`s law and values are listed in Table 2.

$$\text{Degradation Percentage } (\omega) = \left(\frac{C_0 - C_t}{C_0}\right) * 100 \qquad (2)$$

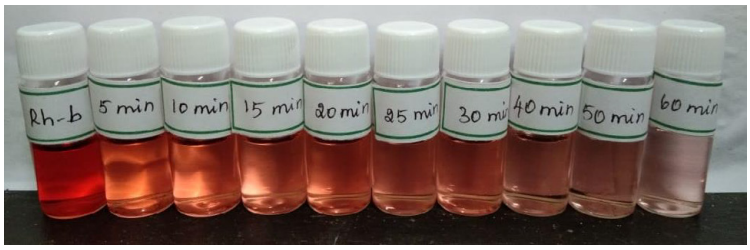

Fig.6 Rh-B dye Adsorption with synthesized C NPs:: Concentrations of the solutions

Table 2. Percentage of degradation of Rh-B dye through adsorption and photocatalytic activity

S.No.	Time (in min)	Adsorption Activity			Photo catalytic Activity		
		C	ω	-ln C/C$_0$	C	ω	-ln C/C$_0$
1	0	100	0	0	100	0	0
2	5	23.17	76.83	1.46	26.9	73.10	1.31
3	10	20.13	79.87	1.60	24.63	75.37	1.40
4	15	19.31	80.69	1.64	21.81	78.19	1.52
5	20	17.58	82.42	1.74	19.81	80.19	1.62
6	25	14.49	85.51	1.93	17.45	82.55	1.75
7	30	10.09	89.91	2.29	14.81	85.19	1.91
8	40	6.77	93.23	2.69	12.36	87.64	2.09
9	50	4.63	95.37	3.07	10.40	89.60	2.26
10	60	3.00	97.00	3.51	5.91	94.09	2.83

where C_0 – initial concentration of dye solution,

C_t – concentration of dye with respect to time t.

It is concluded that the reduction in the concentration of the dye up to 97% of the initial concentration was due to the adsorption of Rh-B dye pollutants by the carbon NPs.

Photocatalytic degradation of dye pollutant by Carbon NPs

The solution containing Rh-B and the carbon NP was exposed to UV irradiation by using fluorescent lamps for the photocatalytic degradation of the dye molecule. Now, 75 mL of the Rh-B dye solution with 5 ppm concentration was sonicated continuously with 5mg of carbon nanoparticle in a 100 mL cylindrical Pyrex vessel reactor. This reaction was initiated by energizing the light source. During this process, for 1 hour at a regular time interval (every 5 min), a 5ml of dye solution, resulting in 10 solution samples. To examine the degradation of Rh-B, the UV-Vis spectra of the collected samples were recorded in an air atmosphere at room temperature by using a UV-Vis spectrometer. Under UV-light irradiation, the photocatalytic performance of the synthesized carbon NPs was examined by the degradation of Rh-B dye molecules [30]. Similar to the adsorption study, here also, the photocatalytic degradation peaks are illustrated in Fig. 7. From these spectra, the intensity of the characteristic peak of Rh-B observed at 500nm decreases with respect to the time for the synthesized carbon NPs. At first, i.e. after 5 minutes the concentration of the dye solution is 26.9% and the absorbance maximum is 0.592 (Table 1). But this value constantly decreases for every 5 minutes time interval. It reaches 0.130 after 60 minutes and the concentration is 5.91%.

It is observed that, for the same time interval of examination as adsorption, 94% of the initial concentration (Table 2) has been reduced due to the photocatalytic degradation of Rh-B dye pollutant by the synthesized carbon NPs.

KINETICS

Fig. 8 showed the time course of Rh-B degradation on synthesized carbon NPs by adsorption and photocatalytic degradation

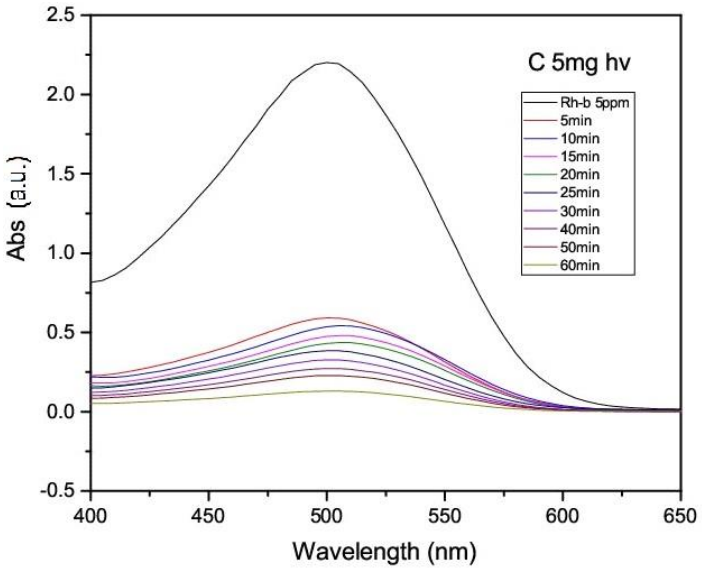

Fig.7 UV – Visible spectra of Rh-B with C NPs at a time interval of 5 minutes from 0 to 60 minutes

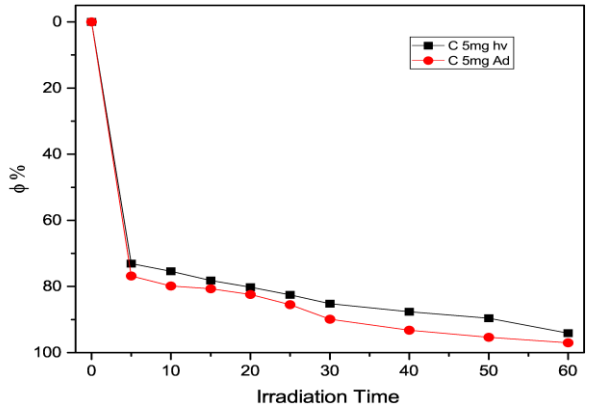

Fig. 8 Time course of Rh-B adsorption on Carbon NPs for both adsorption and photocatalytic degradation

processes respectively. Based on the UV irradiation time intervals, as clearly highlighted in Fig. 8, the adsorption process has significantly degraded the Rh-B due to C NP's nano size, high porous structures, in terms of area, pore-volume, and pore distribution, as compared to the photocatalytic process results. The adsorption equilibrium was achieved after 40 min. The graph matches the physical adsorption curve of Longmuir. But in the photo catalysis process, the low performance of degradation compared to the adsorption process may be due to the rise in temperature bypassing the light radiation. This may cause a desorption process. So, the C NPs act as a better adsorbent than the photo catalytic degrader.

CONCLUSION

As the world's 2nd largest populated country, the paper and textile industries are growing in number. Hence, a huge amount of water resources are contaminated by the discharge of dyes used in those industries. The removal of Rh-B which is one of the commonly used industrial dyes, with carbon NPs synthesized from neem leaves as adsorbent has been experimented with. The proposed adsorption method has significant removal efficiency of up to 97% in minimal time i.e., 60 minutes, and also the synthesis of carbon NPs is cost-effective. Hence, this can be adopted in the industries for the waste water treatment process.

CONFLICTS OF INTEREST

The authors declare that there are no conflicts of interest regarding the publication of this paper.

ACKNOWLEDGMENT

This work was supported by the 2019 TNSCST-S&T Project Grant (Ref.No.TNSCST/STP/AR/2018-2019/9298) from Tamil Nadu State Council for Science and Technology, Chennai. The author acknowledges TNSCST, Chennai for extending financial support. Also, the authors extend sincere thanks to Kalasalingam Academy of Research and Education, Krishnankoil for supporting XRD and SEM analysis and the author's institution for providing necessary infrastructures to carry out this work.

REFERENCES

1.Hunger K. 2007. Industrial Dyes: Chemistry, Properties, Applications, John Wiley & Sons.

2.Rajeev J., Nidhi S., Meenakshi B.,2003 Electromagnetic degradation of Rhodomine Dye in textile and Paper industry effluent. Journal of Scientific and Industrial research, Vo1.62, pp.1138-1144.

3. Pang YL, Lim S, Ong HC, Chong WT. Synthesis, characteristics and sonocatalytic activities of calcined γ-Fe2O3 and TiO2 nanotubes/γ-Fe2O3 magnetic catalysts in the degradation of Orange G. Ultrasonics Sonochemistry. 2016;29:317-27.

4. Rani S, Aggarwal M, Kumar M, Sharma S, Kumar D. Removal of methylene blue and rhodamine B from water by zirconium oxide/graphene. Water Science. 2016;30(1):51-60.

5. Saruchi, Kumar V. Adsorption kinetics and isotherms for the removal of rhodamine B dye and Pb+2 ions from aqueous solutions by a hybrid ion-exchanger. Arabian Journal of Chemistry. 2019;12(3):316-29.

6. Sihem A, Brahmia I, Bousbaa L. Experimental Study of Removal of Rhodamine B by an Activated Cereal by Product. Energy Procedia. 2012;18:1208-19.

7. Zhang Z, Kong J. Novel magnetic Fe3O4@C nanoparticles as adsorbents for removal of organic dyes from aqueous solution. Journal of Hazardous Materials. 2011;193:325-9.

8. Yang N, Zhu S, Zhang D, Xu S. Synthesis and properties of magnetic Fe3O4-activated carbon nanocomposite particles for dye removal. Materials Letters. 2008;62(4-5):645-7.

9. Rajabi HR, Arjmand H, Hoseini SJ, Nasrabadi H. Surface modified magnetic nanoparticles as efficient and green sorbents: Synthesis, characterization, and application for the removal of anionic dye. Journal of Magnetism and Magnetic Materials. 2015;394:7-13.

10. Pengthamkeerati P, Satapanajaru T, Chatsatapattayakul N, Chairattanamanokorn P, Sananwai N. Alkaline treatment of biomass fly ash for reactive dye removal from aqueous solution. Desalination. 2010;261(1-2):34-40.

11. Jiang T, Liang Y-d, He Y-j, Wang Q. Activated carbon/NiFe2O4 magnetic composite: A magnetic adsorbent for the adsorption of methyl orange. Journal of Environmental Chemical Engineering. 2015;3(3):1740-51.

12.Latif A., Noor S., Sharif Q. M., and Najeebullah M.,2010. Different techniques recently used for the treatment of textile dyeing effluents: a review. Journal of the Chemical Society of Pakistan, Vol. 32, No. 1, pp.115–124.

13.Aref Shokri, Kazem Mahanpoor, 2016. Removal of Ortho-Toluidine from Industrial Wastewater by UV/TiO2 Process, Journal of Chemical Health Risks, Vol.6, No.3, 213-223..

14. Giri SK, Das NN, Pradhan GC. Synthesis and characterization of magnetite nanoparticles using waste iron ore tailings for adsorptive removal of dyes from aqueous solution. Colloids and Surfaces A: Physicochemical and Engineering Aspects. 2011;389(1-3):43-9.

15. Shokri A, Mahanpoor K. Degradation of ortho-toluidine from aqueous solution by the TiO2/O3 process. International Journal of Industrial Chemistry. 2016;8(1):101-8.

16. Mohideen SK, Kaliannan SK, Dammalapati PK. Cow dung powder poisoning. Indian Journal of Critical Care Medicine. 2015;19(11):684-6.

17. Shokri A, Bayat A, Mahanpoor K. Employing Fenton-like process for the remediation of petrochemical wastewater through Box–Behnken design method. DESALINATION AND WATER TREATMENT. 2019;166:135-43.

18.Majid Saghi,, Aref Shokri, Ali Arastehnodeh, Mohammad Khazaeinejad, Atena Nozari, 2018. The photo degradation of methyl red in aqueous solutions by α-Fe2 O3 /SiO2 nano photocatalyst, J. Nanoanalysis., Vol.5, No.3, pp.163-170.

19. Postai DL, Demarchi CA, Zanatta F, Melo DCC, Rodrigues CA. Adsorption of rhodamine B and methylene blue dyes using waste of seeds of Aleurites Moluccana, a low cost adsorbent. Alexandria Engineering Journal. 2016;55(2):1713-23.

20. Zargar B, Parham H, Rezazade M. Fast Removal and Recovery of Methylene Blue by Activated Carbon Modified with Magnetic Iron Oxide Nanoparticles. Journal of the Chinese Chemical Society. 2011;58(5):694-9.

21. Shokri A. A kinetic study and application of electro-Fenton process for the remediation of aqueous environment containing toluene in a batch reactor. Russian Journal of Applied Chemistry. 2017;90(3):452-7.

22. Shokri A, Joshagani AH. Using microwave along with TiO2 for degradation of 4-chloro-2-nitrophenol in aqueous environment. Russian Journal of Applied Chemistry. 2016;89(12):1985-90.

23. Allé PH, Fanou GD, Robert D, Adouby K, Drogui P. Photocatalytic degradation of Rhodamine B dye with TiO2 immobilized on SiC foam using full factorial design. Applied Water Science. 2020;10(9).

24. Ullah H, Viglašová E, Galamboš M. Visible Light-Driven Photocatalytic Rhodamine B Degradation Using CdS Nanorods. Processes. 2021;9(2):263.

25. Rubab M, Bhatti IA, Nadeem N, Shah SAR, Yaseen M, Naz MY, et al. Synthesis and photocatalytic degradation of rhodamine B using ternary zeolite/WO3/Fe3O4 composite. Nanotechnology. 2021;32(34):345705.

26.Rajendrachari, S., Kamacı, Y., Taş, R., Ceylan, Y., Uzun, O., Karaoğlanlı, A. 2019. Antimicrobial Investigation of CuO and ZnO Nanoparticles Prepared by a Rapid Combustion Method. Physical Chemistry Research, 7(4), 799-812.

27.Rajendrachari, S., BE, K.,2020. Biosynthesis of Silver Nanoparticles Using Leaves of Acacia Melanoxylon and their Application as Dopamine and Hydrogen Peroxide Sensors. Physical Chemistry Research, Vol.8, No.1, pp.1-18

28. Shashanka R. Investigation of optical and thermal properties of CuO and ZnO nanoparticles prepared by Crocus Sativus (Saffron) flower extract. Journal of the Iranian Chemical Society. 2020;18(2):415-27.
29. Shashanka R, Esgin H, Yilmaz VM, Caglar Y. Fabrication and characterization of green synthesized ZnO nanoparticle based dye-sensitized solar cells. Journal of Science: Advanced Materials and Devices. 2020;5(2):185-91.
30. Rajendrachari S, Taslimi P, Karaoglanli AC, Uzun O, Alp E, Jayaprakash GK. Photocatalytic degradation of Rhodamine B (RhB) dye in waste water and enzymatic inhibition study using cauliflower shaped ZnO nanoparticles synthesized by a novel One-pot green synthesis method. Arabian Journal of Chemistry. 2021;14(6):103180.